Preprints (www.preprints.org) | NOT PEER-REVIEWED | Posted: 21 November 2022 doi:10.20944/preprints202208.0251.v2

Disclaimer/Publisher's Note: The statements, opinions, and data contained in all publications are solely those of the individual author(s) and contributor(s) and not of MDPI and/or the editor(s). MDPI and/or the editor(s) disclaim responsibility for any injury to people or property resulting from any ideas, methods, instructions, or products referred to in the content.

Sagnac effect with non-zero mass particles and light: the transition from classical to relativistic

Mathieu Rouaud*

Independent Researcher, Boudiguen 29310 Querrien, France
* mathieu137@gmail.com

November 20, 2022

Abstract

On a rotating disk, two particles bounce at the vertices of a regular polygon in opposite directions. On the return to the entry point, a clock measures the time difference, called Sagnac effect. Due to Coriolis effects, the counter-clockwise and clockwise paths are different. The particular case of the slow disk where the two trajectories are very close and almost polygonal is studied. The existence of a transition between a classical and a relativistic regime is proved. An experimental verification is proposed. Although the two Sagnac effects seem analogous, in detail their behavior is quite different.

Keywords: Rotating Disk, Special Relativity, Sagnac, synchronization, metric, Coriolis, transition, classical.

Contents

1 Introduction **2**

2 Classical Sagnac effect **2**
2.1 Trajectories and time difference 2
2.2 Centrifugal and Coriolis forces 3
2.3 Slow disk 4

3 Relativistic Sagnac effect **4**
3.1 Synchronization of clocks 4
3.2 Metric 5
3.3 Trajectories and time difference 6
3.4 Slow disk 8

4 Transition **9**

5 Proposals for experiments **9**
5.1 Particle accelerator 9
5.2 Atom gyrometers 11

6 Discussion **12**

7 Conclusion **13**

References **13**

© 2022 by the author(s). Distributed under a Creative Commons CC BY license.

Preprints (www.preprints.org) | NOT PEER-REVIEWED | Posted: 21 November 2022 doi:10.20944/preprints202208.0251.v2

A Classical **14**

B Relativistic **15**

1 Introduction

The Sagnac effect is studied as well for matter particles as for light. The Sagnac effect has been experimentally verified with light, but also with all kinds of particles like neutrons, electrons or atoms. The classical study, as on the example of a child on a merry-go-round with a ball, allows to grasp an origin of the effect. For a rigorous study, paths in the shape of n-sided regular polygons are considered. A circular contour is not directly envisaged because it is not experimentally feasible with particles or light rays. A free particle does not follow a circular path. The circle can be approached but the approximation is not obvious and contains ambiguities. For example, in an optical fiber placed on the rim of a rotating disk, the trajectory is a broken line for a step index fiber, or undulates on both sides of the circular axis for a graded index fiber. Moreover, the historical experiment of Georges Sagnac in 1913 was carried out according to a polygonal contour [1], and most of the current gyrolasers, used daily in aeronautics for navigation, are made of a triangular laser cavity. We show that the trajectory in the direction of rotation is not the same as the one in the opposite direction, both for light and matter, which explains the difference in time to make a turn. The study starts with the case where the disk and the particle are classical. Wave or quantum aspects are only considered in Section 5.

2 Classical Sagnac effect

As is appropriate, light will be studied later in the relativistic framework.

2.1 Trajectories and time difference

In the inertial reference frame R' of the laboratory, where the disk is rotating with the angular frequency ω, we consider a Cartesian system of coordinates (O', x', y', z'). At the instant $t' = 0$, the particle is at the position $A_1 = (r, 0, 0)$ with an initial velocity $\vec{v}'$ orthogonal to the rotation axis $(O'z')$. On figures 1 and 2, the quantities are defined.

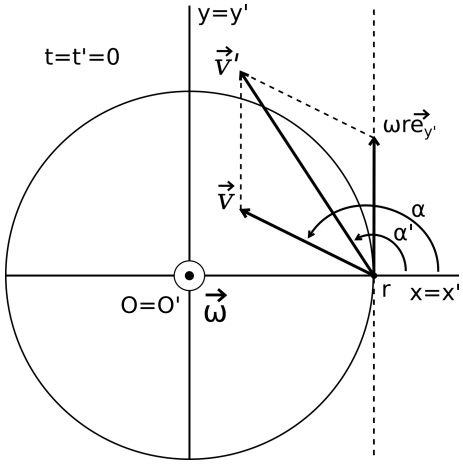

Figure 1: $\alpha, \alpha' \in]\frac{\pi}{2}, \frac{3\pi}{2}[$

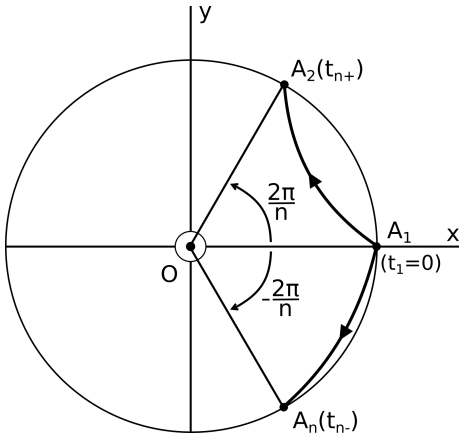

Figure 2: $t_\pm = nt_{n\pm}$
Sagnac effect: $\Delta t = t_+ - t_-$

Preprints (www.preprints.org) | NOT PEER-REVIEWED | Posted: 21 November 2022 doi:10.20944/preprints202208.0251.v2

For a free particle we then have a rectilinear trajectory:

$$x' = v' \cos\alpha' t' + r, \quad y' = v' \sin\alpha' t' \quad \text{and} \quad z' = 0 \tag{1}$$

The non-inertial reference frame of the disk is denoted R with the coordinates (O, x, y, z). The center of the disk is $O = O'$, and at the date $t = 0$, $(O, x) = (O', x')$. We have the following change of polar coordinates for a counterclockwise rotating disk:

$$\rho = \rho', \quad \theta = \theta' - \omega t', \quad z = z' \quad \text{and} \quad t = t' \tag{2}$$

On the disk, from A_1, we throw at $t = 0$ the particle with the speed v and the direction α. The additivity of velocities give the initial quantities v' and α' in R':

$$\vec{v}' = \vec{v} + \vec{v}_{A_1/R'} \quad \Rightarrow \quad v' \cos\alpha' = v\cos\alpha, \quad v' \sin\alpha' = v \sin\alpha + \omega r$$
$$\text{and} \quad v' = v\sqrt{\cos^2\alpha + \left(\sin\alpha + \frac{\omega r}{v}\right)^2}, \quad \alpha' = \arctan\left(\frac{\sin\alpha + \frac{\omega r}{v}}{\cos\alpha}\right) + \pi \tag{3}$$

Then, for $t \in [0, t_n]$, we obtain the trajectory on the disk frame:

$$\rho = \sqrt{(v\cos\alpha t + r)^2 + (v\sin\alpha + \omega r)^2 t^2}$$
$$\text{and} \quad \theta = \arctan\left(\frac{(v\sin\alpha + \omega r)t}{v\cos\alpha t + r}\right) - \omega t + k\pi, \quad k \in \mathbb{Z} \tag{4}$$

On figures 3 and 4, with Eq. 4, the difference of trajectories is shown for $r = 2\,\text{m}$, a period $T = 120\,\text{s}$, an initial speed $v = 0.3\,\text{m/s}$ and different values of n.

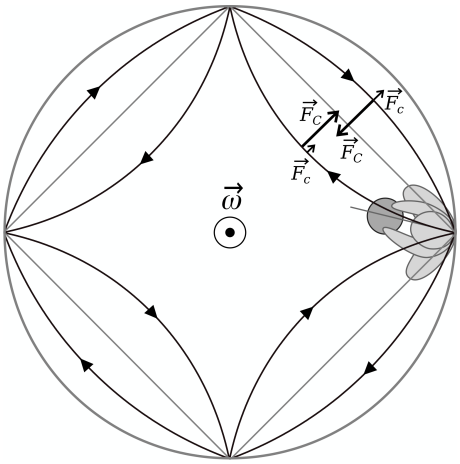

Figure 3: $n = 4$. $\Delta t \simeq 1.9\,\text{s}$.

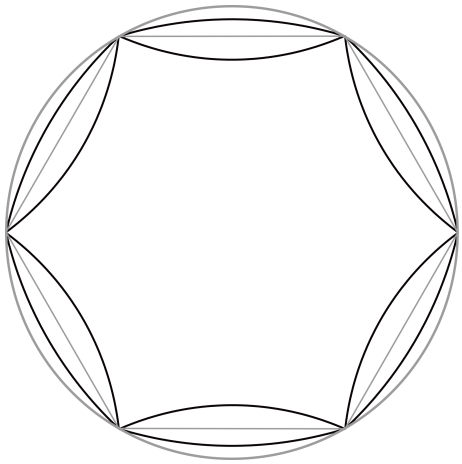

Figure 4: $n = 6$. $\Delta t \simeq 1.1\,\text{s}$.

A child with a ball on a merry-go-round can easily measure the classical Sagnac effect.

2.2 Centrifugal and Coriolis forces

The curved trajectory in the non-inertial frame can be understood by the action of fictitious forces. Centrifugal force $\vec{F}_c$ and Coriolis force $\vec{F}_C$:

$$\vec{F}_c = -m\vec{a}_c, \quad \vec{F}_C = -m\vec{a}_C \quad \text{with} \quad \vec{a}_c = -\omega^2\overrightarrow{OM} \quad \text{and} \quad \vec{a}_C = 2\vec{\omega} \wedge \vec{v} \tag{5}$$

For the counterclockwise rotating disk, second Newton's law give the differential equations:

$$\ddot{\rho} = \rho(\omega + \dot{\theta})^2 \quad \text{and} \quad \rho\ddot{\theta} + 2\dot{\rho}(\omega + \dot{\theta}) = 0 \tag{6}$$

Preprints (www.preprints.org) | NOT PEER-REVIEWED | Posted: 21 November 2022 doi:10.20944/preprints202208.0251.v2

2.3 Slow disk

If the particle speed v' is large compared to the disk speed ωr the trajectories are close to a succession of straight lines. We have $\rho(t_{n\pm}) = r$ and $\theta(t_{n\pm}) = \pm 2\pi/n$, then we perform a series expansion on ωt_n, and we obtain an analytical expression of Δt (Appendix A):

$$t_{n\pm} \simeq \frac{2r\sin\frac{\pi}{n}}{v} + \frac{r\sin\frac{\pi}{n}}{2v}\omega^2 t_n^2 \pm \frac{r\cos\frac{\pi}{n}}{3v}\omega^3 t_n^3 \quad \text{and} \quad \Delta t \simeq \frac{16}{3}\frac{\omega^3 r^4}{v^4} n\cos\frac{\pi}{n}\sin^3\frac{\pi}{n} \qquad (7)$$

The order zero term of the $t = nt_n$ expansion is L_n/v, where $L_n = 2nr\sin(\pi/n)$ is the perimeter of the polygon. There is no order one term. The order two term is the same for counterclockwise and clockwise particles. So, only the third order contribute to the classical Sagnac effect Δt. A first order term would have been proportional to ωA_n, where $A_n = nr^2\sin(\pi/n)\cos(\pi/n)$ is the polygon area. As we will see, it is the case for the relativistic Sagnac effect. Thus, although at a first sight the classical and relativistic effects are analogs, in the details theirs natures are quite different. Also, at the circle limit, when n tends to infinite, the classical Sagnac effect tends to zero, when the relativistic one tends to a non-null limit.

3 Relativistic Sagnac effect

3.1 Synchronization of clocks

The clocks in the inertial frame R' are easily synchronized with Einstein's synchronization method [3]. In the non-inertial disk reference frame R, the proper clocks cannot be synchronized because they have different rates depending on the radial distance ρ. But, as the reference frame of the disk is *stationary*, we can use *coordinate clocks* [4]. We imagine a continuous set of infinitesimal observers who remain at rest on the disk, and each equipped with a ruler, a proper clock and a coordinate clock. First, we synchronized the O's proper clock with the coinciding O''s clock. This is possible, if we assume the following *clock hypothesis*: two clocks at the same speed, whatever their acceleration or spin, undergo the same time dilation. Afterwards, O's clock is our master clock used to synchronize all the coordinate clocks, so we have $t = t'$. This works with a *radar method* if we assume the round-trip symmetric (demonstration given in section 3.3).

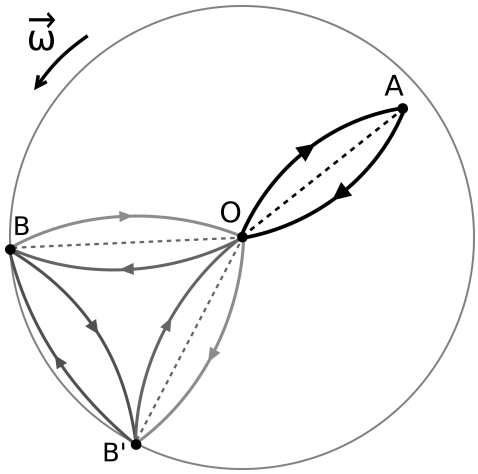

Figure 5: If the round-trip of the light rays is symmetric $\Delta t_{OA} = \Delta t_{AO}$, and all the coordinate clocks on the disk can be synchronized with O's proper clock. Unlike the coordinate clocks B and B', which although located at the same radial distance and therefore at the same rhythm, cannot be directly synchronized because $\Delta t_{BB'} \neq \Delta t_{B'B}$. On the other hand, the synchronization can be done via O where a mirror is placed.

O emits a periodic light signal, and each of the other observers equals the rate of his coordinate clock with the signal received from O. O sends a signal at t_1 reflected by A

Preprints (www.preprints.org) | NOT PEER-REVIEWED | Posted: 21 November 2022 doi:10.20944/preprints202208.0251.v2

(figure 5), and back to O at t_2. When the signal is reflected by A, the time $t = (t_1 + t_2)/2$ is assigned to his coordinate clock. A coordinate clock can be compared to a clock radio-controlled by O's proper clock.

3.2 Metric

Due to symmetries, we assume the following general form for the metric in the disk reference system:

$$ds^2 = g_{\mu\nu}dx^\mu dx^\nu = g_{00}c^2dt^2 + g_{11}d\rho^2 + 2g_{02}cdtd\theta + g_{22}d\theta^2 - dz^2 \tag{8}$$

In the inertial frame:

$$ds'^2 = g'_{\mu\nu}dx'^\mu dx'^\nu = c^2dt'^2 - d\rho'^2 - \rho'^2d\theta'^2 - dz'^2 \tag{9}$$

- According Einstein's conjecture, we have no length contraction along the radial direction, then $\rho = \rho'$ and $g_{11} = -1$.
- For a particle at rest in R, $ds^2 = g_{00}c^2dt^2 = ds'^2 = c^2dt'^2 - dl'^2$, then, with $t = t'$, $\rho' = cst$ and ${\beta_D}'c = {v_D}' = dl'/dt'$ the disk speed in R', $g_{00} = 1 - {\beta_D}'^2 = 1/{\gamma_D}'^2$.
- For a particle at rest in R', $ds'^2 = c^2dt'^2 = ds^2 = g_{00}c^2dt^2 + 2g_{02}cdtd\theta + g_{22}d\theta^2$. For observers placed at the center of the disk, one at rest in R' and the other in R: $\omega' = d\theta'/dt' = -d\theta/dt = \omega$. Then $\omega^2/c^2\ g_{22} = 2\omega/c\ g_{02} + {\beta_D}'^2$.
- Einstein's conjecture illustrated by Ehrenfest's paradox, gives for a circle centered on O, the ratio perimeter/diameter $P/D = \gamma_D\pi$. From the spatial metric $\gamma_{ij} = -g_{ij} + g_{0i}g_{0j}/g_{00}$ [3], $P = \int \sqrt{\gamma_{22}}d\theta$, $D = 2\int \sqrt{\gamma_{11}}d\rho$, and $\omega^2/c^2g_{22} = {\gamma_D}'^2\omega^2/c^2g_{02}^2 - {\gamma_D}^2R^2$.

With $\gamma_D = {\gamma_D}'$, we find the well-known metric in the rotating disk [3]:

$$ds^2 = (1 - {\beta_D}^2)c^2dt^2 - d\rho^2 - 2\omega\rho^2dtd\theta - \rho^2d\theta^2 - dz^2 \quad \text{with} \quad \beta_D(\rho) = \rho\omega/c. \tag{10}$$

We use the Lagrangian approach

$$ds^2 = c^2d\tau^2, \quad \tau = \int L(\rho, \theta, \dot\rho, \dot\theta)dt, \quad \frac{\partial L}{\partial \rho} - \frac{d}{dt}\frac{\partial L}{\partial \dot\rho} = 0 \quad \text{and} \quad \frac{d}{dt}\frac{\partial L}{\partial \dot\theta} = 0 \tag{11}$$

to determine the equations of motion

$$\ddot\rho = \rho(\omega + \dot\theta)^2 \quad \text{and} \quad \rho\ddot\theta + 2\dot\rho(\omega + \dot\theta) = 0. \tag{12}$$

In relativity, the inertial forces are replaced by metric effects. In a non-inertial reference frame, we no longer have a Minkowskian metric and a free particle follows a geodesic which modifies its initially rectilinear and uniform motion to follow a curved and accelerated trajectory.

It is also interesting to note that the following change of coordinate give the same metric 10 from the metric 9 in the inertial frame:

$$\rho = \rho', \quad \theta = \theta' - \omega t', \quad z = z' \quad \text{and} \quad t = t'. \tag{13}$$

Eventually, the equations of motion and the change of coordinates are the same for the classical and relativistic theories. The similarity is only apparent, although the trajectories are the same for the same initial speed in the disk, the absolute time is replaced by the coordinate time. Moreover, due to different velocity composition laws, the velocity of the particle in the inertial reference frame is not the same.

Preprints (www.preprints.org) | NOT PEER-REVIEWED | Posted: 21 November 2022 doi:10.20944/preprints202208.0251.v2

3.3 Trajectories and time difference

On the disk, from A_1, we throw at $t = 0$ the particle with the speed v and the direction α. The law of composition of velocities gives a relation between the velocities measured by two inertial observers. One observer is at rest in R', but the second observer cannot be the one at rest on the disk, because the disk frame is not inertial. So we choose the inertial reference frame coinciding locally at A_1 and $t = 0$, because, according to the *equivalence principle*, for any space-time event there is, locally, a coinciding inertial reference frame. This local Minkowskian observer, and the neighboring observers, use their standard rulers and proper clocks to measure the local velocity: $v_{loc} = dl/dt_{loc}$ with $dt_{loc} = d\tau$. Whereas the non-inertial observer coinciding at rest on the disk, uses his coordinate clock and obtains the coordinate velocity: $v = v_{coord} = dl/dt_{coord}$, $dt_{coord} = dt = \gamma_D d\tau$ according metric 10, and $v_{loc} = \gamma_D v$. Considering all of the above, the composition of velocities give the initial quantities v' and α' in R':

$$\begin{aligned}\vec{v'} &= \left(\frac{(v_x)_{loc}}{\gamma_D(1+\beta_D(v_y)_{loc}/c)}, \frac{(v_y)_{loc}+\omega r}{1+\beta_D(v_y)_{loc}/c}\right) \\ &= \left(\frac{v\cos\alpha}{1+\beta_D\gamma_D v\sin\alpha/c}, \frac{\gamma_D v\sin\alpha + c\beta_D}{1+\beta_D\gamma_D v\sin\alpha/c}\right) = \left(v'\cos\alpha', v'\sin\alpha'\right) \\ \text{and} \quad v' &= v\frac{\sqrt{\cos^2\alpha + \left(\gamma_D\sin\alpha + \frac{\omega r}{v}\right)^2}}{1+\beta_D\gamma_D v\sin\alpha/c}, \quad \alpha' = \arctan\left(\frac{\gamma_D\sin\alpha + \frac{\omega r}{v}}{\cos\alpha}\right) + \pi \end{aligned} \tag{14}$$

Then, for $t \in [0, t_n]$, we obtain the trajectory on the disk frame:

$$\begin{aligned}\rho &= \frac{\sqrt{[v\cos\alpha t + r(1+\beta_D\gamma_D v\sin\alpha/c)]^2 + (\gamma_D v\sin\alpha + c\beta_D)^2 t^2}}{1+\beta_D\gamma_D v\sin\alpha/c} \\ \text{and} \quad \theta &= \arctan\left(\frac{(\gamma_D v\sin\alpha + c\beta_D)t}{v\cos\alpha t + r(1+\beta_D\gamma_D v\sin\alpha/c)}\right) - \omega t + k\pi, \quad k \in \mathbb{Z}\end{aligned} \tag{15}$$

We can now plot the trajectories for all particles and all rotation speeds. In figure 6, the disk reaches relativistic velocities, these two examples allow to understand fundamental aspects of the theory. Certainly some physical limitations are imposed on the rotation speed of the disk. But, even if, the disk can barely have a tiny portion of the speed c (the maximum disk speed is close to the speed of sound in the disk material), it is important to know the behavior of a particle close to the maximum value $r_{max} = c/\omega$ seen from an observer at rest on the disk.

Preprints (www.preprints.org) | NOT PEER-REVIEWED | Posted: 21 November 2022 doi:10.20944/preprints202208.0251.v2

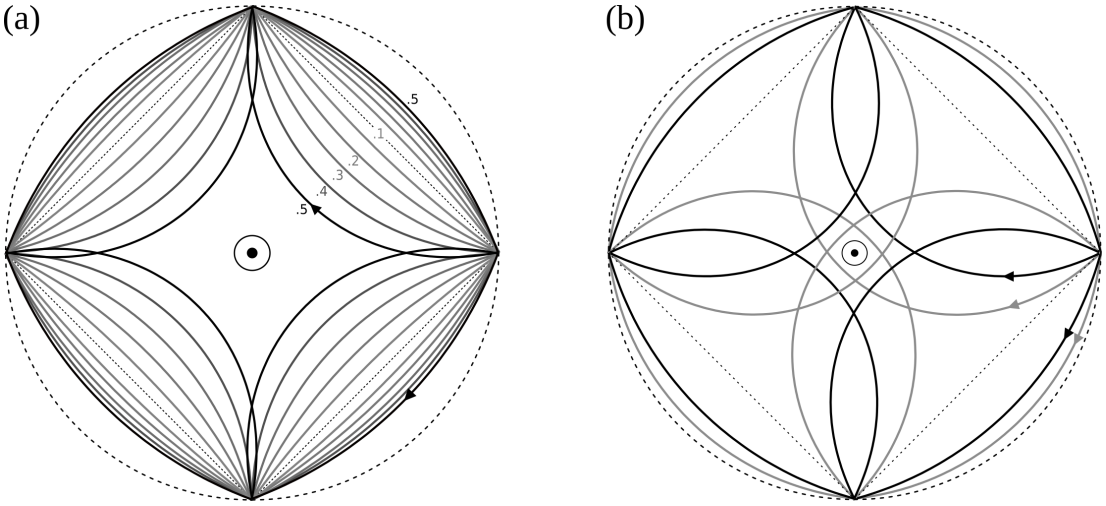

Figure 6: **(a)** Light. Even for a ray of light, the trajectories in opposite directions are not the same. The counterclockwise A_+ and clockwise A_- areas are different (if $A_+ \subset A_-$ then $A_+ < A_-$), and the well-known formula $\Delta\tau = 4\omega A/c^2$ cannot work. Examples: disk with a speed of 50%, 40%, 30%, 20% and 10% of c on the rim in the laboratory. Sagnac effect for $r = 2$ m: $\Delta\tau \simeq 21, 18, 15, 10$ and 5.2 ns. With the formula $\Delta\tau = 4\omega A/c^2 \simeq 27, 21, 16, 11$ and 5.3 ns. **(b)** Relativistic particle with a 95%c initial local speed in the disk frame and a disk with a speed of 60%c on the rim in the laboratory. Classical case in gray. Even if the equations of motion are the same, the trajectories are different. Sagnac effect for $r = 2$ m: $\Delta t_{coord} \simeq 28$ ns, $\Delta t_{loc} = \Delta\tau \simeq 22$ ns, classical $\Delta t \simeq 34$ ns.

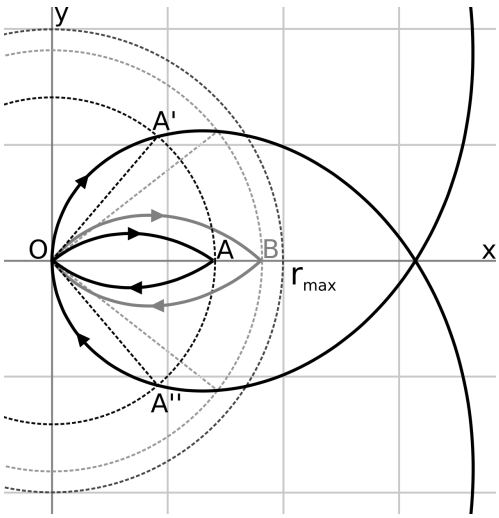

Figure 7: Light, $v = c$ at O. $\Delta t_{OA} = \Delta t_{AO} = r/c$

.

Preprints (www.preprints.org) | NOT PEER-REVIEWED | Posted: 21 November 2022 doi:10.20944/preprints202208.0251.v2

We can now demonstrate that the round-trip of the light rays is symmetric between O and A in figure 5. Let us take in R' the trajectory of a particle along the $O'y'$ axis. The particle passes in O' at $t = 0$ and for the initial velocity $v' = v$ (figure 7). For $t \geqslant 0$, $\theta' = +\pi/2$, $\rho = vt$ and $\theta = \pi/2 - \omega\rho/v$. For $t < 0$, $\theta' = -\pi/2$, $\rho = -vt$ and $\theta = -\pi/2 + \omega\rho/v$. So we have $\rho = v/\omega(\pi/2 \mp \theta)$, $\rho(\theta) = \rho(-\theta)$ and $t(\theta) = -t(-\theta)$.

3.4 Slow disk

If the particle speed v' is large compared to the disk speed ωr the trajectories are close to a succession of straight lines. We have $\rho(t_{n\pm}) = r$ and $\theta(t_{n\pm}) = \pm 2\pi/n$ and we perform a series expansion on $\epsilon = \omega r/v$. Indeed $v \simeq v'$ and $\epsilon << 1$. We obtain an analytical expression of Δt with $\beta_c = v/c$ (Appendix B):

$$\begin{aligned}\omega t_{n\pm} = {} & 2\epsilon \sin\frac{\pi}{n} \pm 2\epsilon^2 \sin\frac{\pi}{n}\cos\frac{\pi}{n} \\ & + \epsilon^3 \sin\frac{\pi}{n}\left[2\sin^2\frac{\pi}{n} + {\beta_c}^2\left(1 - 5\sin^2\frac{\pi}{n}\right)\right] \\ & \pm 2\epsilon^4 \sin\frac{\pi}{n}\cos\frac{\pi}{n}\left[\frac{4}{3}\sin^2\frac{\pi}{n} - 2{\beta_c}^2\sin^2\frac{\pi}{n} + {\beta_c}^4\left(1 - 2\sin^2\frac{\pi}{n}\right)\right] \\ & + o(\epsilon^5)\end{aligned} \tag{16}$$

Coordinate time difference for the slow disk:

$$\Delta t \simeq 4\frac{\omega A_n}{c^2} + 4\frac{\omega^3 r^2}{v^4} A_n \left[\frac{4}{3}\sin^2\frac{\pi}{n} - 2{\beta_c}^2\sin^2\frac{\pi}{n} + {\beta_c}^4\left(1 - 2\sin^2\frac{\pi}{n}\right)\right] \tag{17}$$

Sagnac effect for the slow disk with $\Delta\tau = \Delta t/\gamma_D$ and $\gamma_D = 1/\sqrt{1 - \epsilon^2{\beta_c}^2}$:

$$\Delta\tau \simeq 4\frac{\omega A_n}{c^2} + 4\frac{\omega^3 r^2}{v^4} A_n \left[\frac{4}{3}\sin^2\frac{\pi}{n} - 2{\beta_c}^2\sin^2\frac{\pi}{n} + {\beta_c}^4\left(\frac{1}{2} - 2\sin^2\frac{\pi}{n}\right)\right] \tag{18}$$

This formula works for all particles. Whether light or matter.

Luminous Sagnac effect for a regular n-polygon with $v = v_{loc}/\gamma_D$ and $v_{loc} = c$:

$$\Delta\tau \simeq 4\frac{\omega A_n}{c^2}\left[1 + \frac{\omega^2 r^2}{c^2}\left(\frac{1}{2} - \frac{8}{3}\sin^2\frac{\pi}{n}\right)\right] \tag{19}$$

Sagnac effect in the limit case of the circle, when n tends to infinity, for both light and matter:

$$\Delta\tau \simeq 4\frac{\omega A}{c^2}\left(1 + \frac{1}{2}\frac{\omega^2 r^2}{c^2}\right) \quad \text{with} \quad A = \pi r^2. \tag{20}$$

For light rays along a circle, we find the same result starting from the metric with $d\tau = 0$ and $\rho = r = cst$ [2]:

$$c^2 d\tau^2 = 0 = (1 - {\beta_D}^2)c^2 dt^2 - c/\omega\, {\beta_D}^2 c dt d\theta - c^2/\omega^2\, {\beta_D}^2 d\theta^2, \tag{21}$$

then $c^2 dt^2 = {\beta_D}^2(cdt + cd\theta/\omega)^2$ and $dt = \pm r d\theta/(c \mp \omega r)$. By integrating counterclockwise and clockwise we find back the circular optic Sagnac effect:

$$\Delta t = t_+ - t_- = 4\frac{\omega A}{c^2}\left(1 - \frac{\omega^2 r^2}{c^2}\right)^{-1} \quad \text{and} \quad \Delta\tau = 4\frac{\omega A}{c^2}\left(1 - \frac{\omega^2 r^2}{c^2}\right)^{-\frac{1}{2}}. \tag{22}$$

Preprints (www.preprints.org) | NOT PEER-REVIEWED | Posted: 21 November 2022 doi:10.20944/preprints202208.0251.v2

4 Transition

In the limit of the slow disk, in formula 18, appears the classical regime ($c \to +\infty$), the relativistic regime ($v_{loc} \to c$) and the transition between the two. In figure 8, for each curve we keep constant the ratio ϵ between the disk speed ωr on the rim and the initial particle coordinate speed v on the disk. In the classical regime the Sagnac effect is inversely proportional to β_c, whereas in the relativistic regime the Sagnac effect is proportional to β_c. At the transition, we obtain a minimal value of $\Delta\tau$:

$$\Delta\tau \quad \text{minimal} \quad \text{for} \quad \beta_{c\,min} = 2/\sqrt{3}\,\epsilon \sin(\pi/n). \tag{23}$$

For a circular path, there is no transition, and the behavior is always relativistic. In the relativistic regime the Sagnac effect is independent of the speed v of the particle. It works for a light ray in a medium or a particle of matter. This is the so called *universality of the Sagnac effect* [7].

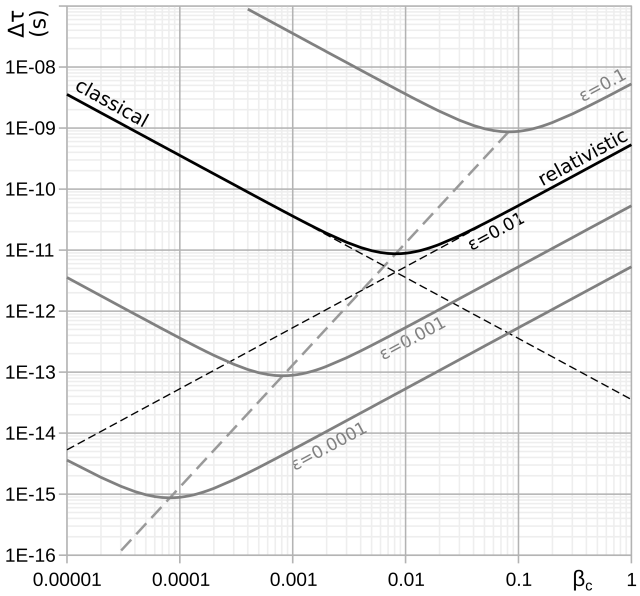

Figure 8: Sagnac Effect, transition from classical to relativistic. Slow disk with $\omega r/v = \epsilon = cst << 1$. Classical limit: $\Delta\tau = (16/3\ \epsilon^3 A_n \sin^2(\pi/n)/rc)/\beta_c$. Relativistic limit: $\Delta\tau = 4\omega A_n/c^2 = (4\epsilon A_n/rc)\beta_c$. Figure for $r = 2$ m and $n = 4$.

5 Proposals for experiments

5.1 Particle accelerator

An experiment to be carried out to highlight the transition between classical and relativistic Sagnac effects. We have a particle gun that allows us to control the velocity of the particles. The rotation speed of the platform is also adjustable. The disk is slow, and in order to maintain the ratio ϵ between the rotating disk speed and the particles velocity, we change the disk angular speed proportionally to the particles speed.

If we use an electron gun, the counterclockwise and clockwise charges will interact electrically at the midpoint, so we can use a neutral particle gun, or send counterclockwise

Preprints (www.preprints.org) | NOT PEER-REVIEWED | Posted: 21 November 2022 doi:10.20944/preprints202208.0251.v2

and clockwise charged particles one after the other.

Finally the simplest way is to have a cyclic particle accelerator placed on a rotating platform (figure 9).

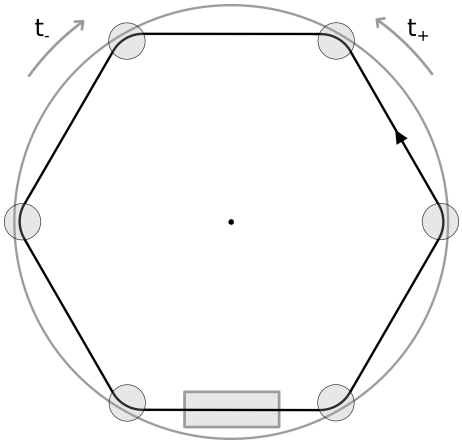

Figure 9: The apparatus uses magnetic fields to bend the charged particle trajectories into a hexagon. The particle speed is controlled and kept constant. The number of revolutions and the time are measured. The particles always travel the polygon in the same direction and it is the platform that changes the direction of rotation for the t_+ and t_- measurements.

In practice, for a disk with a diameter of 4 m which rotates with a speed on the rim 10000 times lower than the speed of the particles, the Sagnac effect is around a femtosecond near the transition. To increase the effect, the particle can make a large number N of turns. On figure 10, $N = 10^6$ and the Sagnac effect is around a nanosecond.

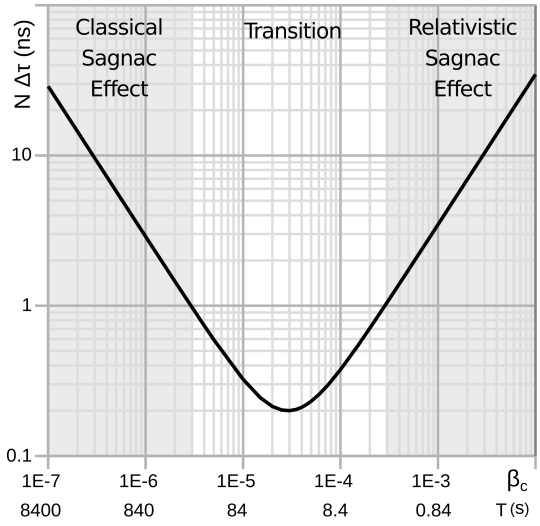

Figure 10: For $r = 2$ m, $n = 6$, $\epsilon = 5 \times 10^{-5}$ and $N = 10^6$.
If $\beta_c = \beta_{cmin} \simeq 2.9 \times 10^{-5}$ then $T \simeq 28$ s, $N\Delta\tau \simeq 0.2$ ns and $Nt \simeq 22$ min.
If $\beta_c = 10\beta_{cmin}$ then $T \simeq 2.8$ s, $N\Delta\tau \simeq 1$ ns and $Nt \simeq 133$ s.
If $\beta_c = \beta_{cmin}/10$ then $T \simeq 280$ s, $N\Delta\tau \simeq 1$ ns and $Nt \simeq 3.7$ h.

In the relativistic regime the disk rotates faster and one can wonder if the centrifugal force does not deform the platform too much. Indeed the platform is not perfectly rigid and we have to consider the mechanical constraints exerted on the disk by the acceleration. We model the disk by a homogeneous cylinder of density ρ and modulus of rigidity E. According to Hooke's law $\sigma = E\epsilon$ with σ the pressure exerted and $\epsilon = \Delta l/l$ the relative deformation. Due to its elasticity, the disk becomes wider and its radius increases. We calculate the extension by integrating over the entire disk and we find $\Delta r = \rho\omega^2 r^3/9E$. Fortunately, the consequences on the Sagnac effect are negligible. For example on figure 10, with a marble platform, if we consider the relativistic regime with $\beta_c = 10^{-3}$ and $T = 0.84$ s, then $\Delta r \simeq 5$ μm, and $\Delta\tau$ remains almost the same with $N\Delta\tau \simeq 3.47$ ns.

Preprints (www.preprints.org) | NOT PEER-REVIEWED | Posted: 21 November 2022 doi:10.20944/preprints202208.0251.v2

5.2 Atom gyrometers

With the current progress of atom lasers, we can propose another experiment. In the Sagnac experiment, instead of looking at the difference in time when the rays return, we can consider the wave aspect of light and measure the phase shift. Nowadays, we do the same with atoms that follow two different paths and then interfere in a Mach-Zehnder-type interferometer [11] (figure 11). The inherent sensitivity of atom gyrometers exceeds that of photon gyrometers by several orders of magnitude.

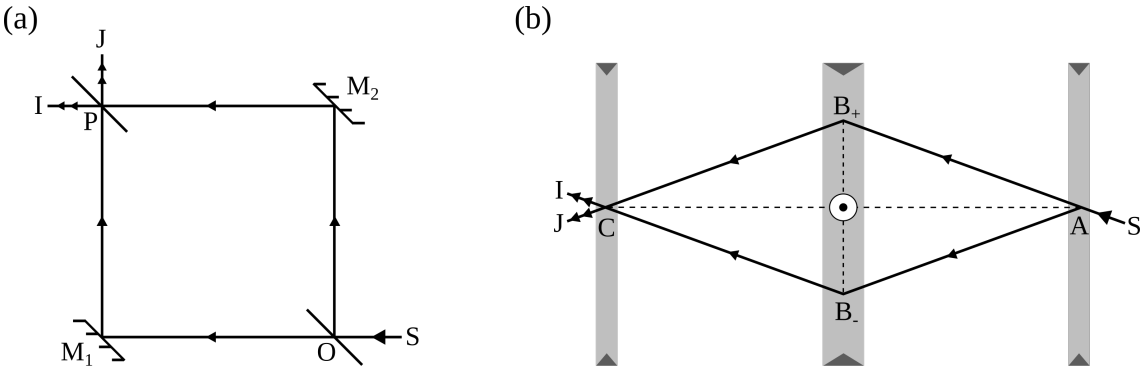

Figure 11: **(a)** Mach-Zehnder interferometer: a coherent light source S, such as a laser, emits a light ray which encounter at O a first half-silvered mirror, so half of the light is transmitted to the mirror M_1, while the other half is reflected by M_2. Both beams recombine at P with the second beam splitter and interfere on the detector I. Due to front-surface reflections the interference is destructive at J. **(b)** Atom interferometer: compared to the traditional optical interferometer (a), light and matter invert their roles. The beam of atoms S is split by a laser into two beams, which after a certain distance are redirected to each other with another laser. Appropriately used lasers act as splitters and mirrors for coherent atomic beams.

In the case below, the path is diamond-shaped, and the light pulses are considered to act as splitters and mirrors (figure 11 (b)). The calculations of subsection 3.4 are resumed with $\rho(t_A = 0) = r_M$, $\rho(t_{B_\pm}) = r_m$ and $\theta(t_{B_\pm}) = \pm\pi/2$. A series expansion on $\epsilon = \omega r_M/v$ is performed. Considering symmetries $\Delta t_{AB} = \Delta t_{BC}$, then:

$$\Delta t \simeq 2\frac{\omega A}{c^2} + \frac{2}{3}\frac{\omega^3 l^2 A}{v^4}\left(1 - \frac{3}{2}{\beta_c}^2\right) \quad \text{with} \quad l = \sqrt{r_M^2 + r_m^2} \tag{24}$$

In the context of the experiments carried out, $v << c$, $\beta_D << 1$ and $\Delta\tau \simeq \Delta t$, so:

$$\Delta\tau \simeq 2\frac{\omega A}{c^2} + \frac{2}{3}\frac{\omega^3 l^2 A}{v^4} \tag{25}$$

Using the result of J. Anandan [12], $\Delta\phi/\pi = (2mc^2/h)\Delta\tau$, then:

$$z = \frac{\Delta\phi}{\pi} \simeq \frac{4m\omega A}{h}\left(1 + \frac{c^2\omega^2 l^2}{3v^4}\right) \tag{26}$$

In figure 12, two curves are plotted and the results of the Lenef *et al* [13] and Gustavson *et al* [14] experiments are compared. The angular rates ω are of the order of the Earth's rotation rate and a phase shift of several fringes is obtained. The Lenef *et al* experiment use a beam of Na atoms with $v \simeq 1030$ m/s, $r_M \simeq 0.66$ m, $r_m \simeq 27,8$ μm, $A \simeq 37$ mm^2, and ω ranges up to 146 μrad/s. The Gustavson *et al* experiment use a beam of Cs atoms with $v \simeq 290$ m/s, $r_M \simeq 0.96$ m, $r_m \simeq 11,5$ μm, $A \simeq 22$ mm^2, and ω ranges up to 145 μrad/s. In this last experiment the transition is approached.

Preprints (www.preprints.org) | NOT PEER-REVIEWED | Posted: 21 November 2022 doi:10.20944/preprints202208.0251.v2

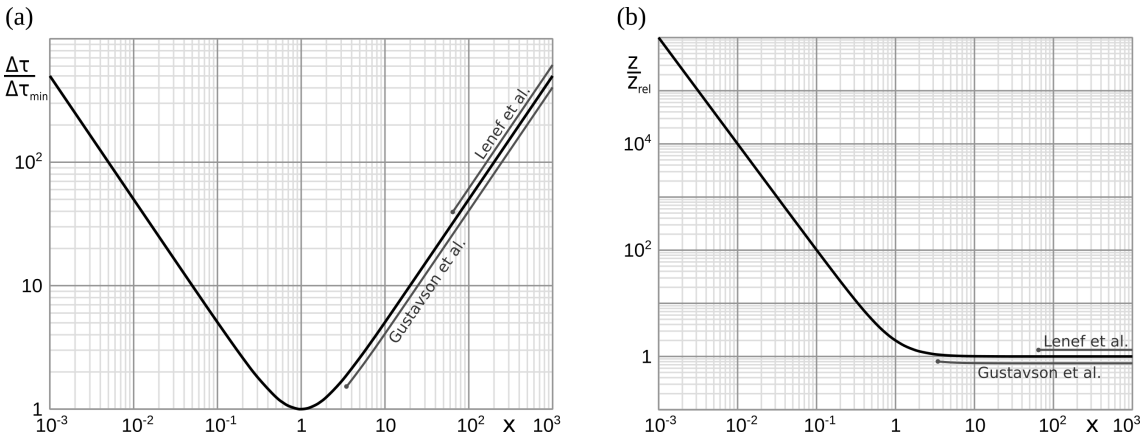

Figure 12: **(a)** Two experiments results represented on the dimensionless curve $\Delta\tau/\Delta\tau_{min}$ versus $x = \beta/\beta_{min}$ with $\beta_{min} = l\epsilon/\sqrt{3}r_M$ and $\Delta\tau/\Delta\tau_{min} = 1/2(x + 1/x)$. **(b)** The fringe shift compared with the relativistic case: $z/z_{rel} = 1 + 1/x^2$ with $z_{rel} = 4m\omega A/h$.

6 Discussion

As indicated in section 3.1, the synchronization of the clocks on the periphery of the disk is not symmetrical. Thus, if we apply the standard protocol of symmetrical radar echoes, we artificially obtain a *time gap* which corresponds in fact to the Sagnac effect. As Dennis Dieks explains [8] "while establishing standard simultaneity along the way, we create a 'time gap' [...] This is the celebrated Sagnac effect". We have a full synchronization on the disk which works perfectly, and the rigid space-filling *lattice* is permanently synchronized with the master clock [4].

With our coordinate system on the rotating disk, we cannot study the case where $\rho > r_{max}$. This is only an artifact due to the fact that the coordinate system is built with the help of clocks at rest on the disk. But the disk cannot have a physical existence beyond r_{max}. Nevertheless it goes without saying that the particle exists beyond r_{max}, we see it in the inertial reference frame where the trajectory is rectilinear, uniform and infinite.

In subsection 3.2, we assume that $\gamma_D = \gamma_D{}'$. However, these are two quantities of distinct natures, and, *a priori*, different. γ_D represents the curvature of space, proper to R, while $\gamma_D{}'$ represents the time dilation between two inertial reference frames, R_{loc} and R'. On the other hand, the $\gamma_D = \gamma_D{}'$ assumption is quite logical because the reasoning of the Ehrenfest's paradox is based on local inertial reference frames and in this case the length contraction factor equals the time dilation factor. The experiment proposed in Section 5 can be an opportunity to verify this hypothesis.

Note that, as set in subsection 3.2, $\gamma_D{}' = 1/\sqrt{1 - \beta_D{}'^2}$ with $\beta_D{}'c = v_D{}' = w'\rho' = w\rho$ the disk speed with respect to the laboratory at $\rho' = \rho$, but, *a priori*, the laboratory speed v_D with respect to the disk at ρ is different: $v_D \neq v_D{}'$. Indeed, for an observer at rest at ρ on the disk, the laboratory make one revolution of distance $2\pi\rho\gamma_D$ during $\tau = T/\gamma_D{}'$ then the speed measured locally is $v_{D\,loc} = \gamma_D\gamma_D{}'v_D{}'$, the coordinate speed is $v_D = \gamma_D v_D{}'$, and, with $\gamma_D = \gamma_D{}'$, we obtain $\gamma_D = \sqrt{1 + \beta_D{}^2}$. The observer of the disk sees the laboratory rotating faster than the observer of the laboratory sees the disk rotating, especially as the observers get closer to r_{max}.

We find the limit of the circle from the polygon by applying the assumptions of special relativity (including the principle of local equivalence). We then understand that the trajectory is fundamentally polygonal (and not cicular), and that the counterclockwise

Preprints (www.preprints.org) | NOT PEER-REVIEWED | Posted: 21 November 2022 doi:10.20944/preprints202208.0251.v2

and clockwise trajectories are different. Thus the luminous Sagnac effect does not conflict with the principle of local isotropy of the speed of light as suggested, for example, by Selleri and Klauber [8].

It is sometimes stated that there is no non-relativistic Sagnac effect. This is of course true in the relativistic regime, but by simply considering the Sagnac effect as the difference in travel time of any particle depending on the direction of rotation of the disk, we have proved that the effect also has a classical component. The Sagnac effect was first considered in reference to the historical experiment carried out with light in 1913 by Georges Sagnac [1], the effect has then been generalized for the particles of matter always with $\Delta\tau = 4\omega A/c^2$, but by omitting the classical term of equation 18.

In this article, we study the rotating disk from the point of view of special relativity, we do not talk about general relativity or gravitation, because the Riemann curvature tensor is identically null [10] and the spacetime flat, which is normal because we can switch to an inertial reference frame by a global change of coordinates. But often the rotating disk is treated in the framework of general relativity, for example in Landau's book *The Classical Theory of Fields* [3], the rotating disk is studied in the chapter *Particle in a Gravitational Field*. As in Rindler's book *Relativity, Special, General, and Cosmological* [4], it is dealt with in the chapter *General Relativity*. Same in the book of Møller *The Theory of Relativity* [5]. And especially in Einstein's book *Relativity: the Special and General Theory* [6], which is consistent because the primary goal was to find a guiding thread to build the general relativity. Let us quote Malykin [9]: "the use of [the general theory of relativity] is unnecessary when purely kinematic effects are considered". The two approaches give, of course, the same results, but, in my opinion, it is not justified in this context to use general relativity, it complicates unnecessarily, it hides the simplicity and depth of special relativity, and it can mislead the uninitiated.

7 Conclusion

We have shown that the well known formula of the Sagnac effect $\Delta\tau = 4\omega A/c^2$ corresponds to the time difference of particle paths in opposite directions for a slow disk in the relativistic regime. In the general case we no longer have a closed loop, we have different trajectories conterclockwise and clockwise, and the results differ. Here, the definition of the Sagnac effect has been considered in a broad way including particles of non-zero mass, we then highlight, in the particular case of the regular polygon, two types of behavior and a transition between a slow Sagnac effect which can be explained by classical mechanics and a fast Sagnac effect of relativistic nature. It would be very interesting to conduct experiments to study the transition. The more we know about the theoretical aspects of the Sagnac effect, the better the accuracy of future gyrometers can be.

References

[1] G. Sagnac, *Sur la preuve de la réalité de l'éther lumineux par l'expérience de l'interférographe tournant*, Compt. Rend. **157**, 708, 1410 (1913). English: *Regarding the Proof for the Existence of a Luminiferous Ether Using a Rotating Inteferometer Experiment.*

[2] E. J. Post, *Sagnac effect*, Rev. Mod. Phys. **39**(2), 475 (1967), `https://doi.org/10.1103/RevModPhys.39.475`.

Preprints (www.preprints.org) | NOT PEER-REVIEWED | Posted: 21 November 2022 doi:10.20944/preprints202208.0251.v2

[3] L. Landau and E. Lifchitz, *The classical Theory of Fields*, § Distances and time intervals, § Rotation.

[4] W. Rindler, *Relativity: Special, General, and Cosmological*, Oxford Univ. Press, 2^{nd} Ed. (2006), § Synchronization of clocks.

[5] C. Møller, *The Theory of Relativity* (1952). See p222 in Oxford 1^{st} Ed.

[6] Einstein, A. *Relativity: The Special and General Theory* (1917).

[7] G. Rizzi and M. L. Ruggiero, *A Direct Kinematical Derivation of the Relativistic Sagnac Effect for Light or Matter Beams*, Gen. Relativ. Gravit. **35**, 2129–2136 (2003). https://doi.org/10.1023/A:1027345505786

[8] G. Rizzi and M. L. Ruggiero (ed.), *Relativity in rotating frames: relativistic physics in rotating reference frames*, Springer Science & Business Media, Vol. 135 (2003), ISBN 1-4020-1805-3. See on page 37 and 383.

[9] G. Malykin, The Sagnac effect : correct and incorrect explanations, Phys.-Uspekhi, **43** (12), p. 1229 (2000), https://doi.org/10.1070/PU2000v043n12ABEH000830.

[10] M. Rouaud, *Special Relativity, A Geometric Approach*, ISBN 9782954930930, See p243 (2020), http://www.voyagepourproxima.fr/SR.pdf.

[11] K. Bongs, M. Holynski, J. Vovrosh, P. Bouyer, G. Condon, E. Rasel, C. Schubert, W. Schleich and A. Roura, *Taking atom interferometric quantum sensors from the laboratory to real-world applications*, Nat. Rev. Phys. **1**, 731–739 (2019), https://dx.doi.org/10.1038/s42254-019-0117-4.

[12] J. Anandan, *Sagnac effect in relativistic and nonrelativistic physics*, Phys. Rev. D, **24**, p 338, (1981), https://dx.doi.org/10.1103/PhysRevD.24.338.

[13] A. Lenef, T. D. Hammond, E. T. Smith, M. S. Chapman, R. A. Rubenstein and D. E. Pritchard, *Rotation sensing with an atom interferometer*. Phys. Rev. Lett. **78**(5), 760, (1997), https://doi.org/10.1103/PhysRevLett.78.760.

[14] T. L. Gustavson, P. Bouyer and M. A. Kasevich, *Precision rotation measurements with an atom interferometer gyroscope*. Phys. Rev. Lett. **78**, 2046–2049 (1997), https://doi.org/10.1103/PhysRevLett.78.2046.

A Classical

Slow disk: $v' >> \omega r$, $v \simeq v'$, $T >> nt_n$, $\omega t_n = 2\pi t_n/T << 1$

$$\begin{cases} r^2 = (v\cos\alpha_n t_n + r)^2 + (v\sin\alpha_n + \omega r)^2 {t_n}^2 \\ \tan\theta'_n = \dfrac{y'_n}{x'_n} \quad \Rightarrow \quad \tan\left(\pm 2\pi/n + \omega t_n\right) = \dfrac{(v\sin\alpha_n + \omega r)t_n}{v\cos\alpha_n t_n + r} \end{cases}$$

Preprints (www.preprints.org) | NOT PEER-REVIEWED | Posted: 21 November 2022 doi:10.20944/preprints202208.0251.v2

We eliminate α_n:

$$\begin{cases} \dfrac{v\cos\alpha_n t_n}{r} = \dfrac{1}{\sqrt{1+\tan^2\theta'_n}} - 1 \quad \text{if} \quad n>4 \quad \text{then} \quad x'_n \geqslant 0 \\ \dfrac{v\sin\alpha_n t_n}{r} = \pm\dfrac{1}{\sqrt{1+1/\tan^2\theta'_n}} - \omega t_n \quad \text{if} \quad \text{clockwise} \quad y'_n \geqslant 0 \quad \text{else} \quad y'_n < 0 \end{cases}$$

$$\text{then} \quad \frac{vt_n}{r} = \sqrt{\left(\frac{1}{\sqrt{1+\tan^2\theta'_n}} - 1\right)^2 + \left(\pm\frac{1}{\sqrt{1+1/\tan^2\theta'_n}} - \omega t_n\right)^2}$$

vt_n/r order zero.

$$\frac{1}{\sqrt{1+\tan^2\theta'_n}} = |\cos\theta'_n| = \cos\left(\frac{2\pi}{n}(1\pm x)\right), \quad \text{with} \quad x = \frac{nt_n}{T} << 1 \quad \text{and} \quad x'_n \geqslant 0,$$

$$\text{and} \quad \frac{1}{\sqrt{1+1/\tan^2\theta'_n}} = |\sin\theta'_n| = \sin\left(\frac{2\pi}{n}(1\pm x)\right)$$

If $x'_n < 0$ the signs balance out and we obtain the same expression.

$$\text{then} \quad \frac{vt_n}{r} = \sqrt{\left(\cos\left(\frac{2\pi}{n}(1\pm x)\right) - 1\right)^2 + \left(\pm\sin\left(\frac{2\pi}{n}(1\pm x)\right) - \omega t_n\right)^2}$$

$$= \sqrt{2 - 2\cos\left(\frac{2\pi}{n}(1\pm x)\right) \mp 2\sin\left(\frac{2\pi}{n}(1\pm x)\right)\frac{2\pi}{n}x + \left(\frac{2\pi}{n}\right)^2 x^2}$$

Series expansion on x:

$$\underbrace{\frac{vt_n}{r}}_{\text{order 0}} = \underbrace{2\sin\left(\frac{\pi}{n}\right)}_{\text{order 0}} + \underbrace{2\sin\left(\frac{\pi}{n}\right)\left(\frac{\pi x}{n}\right)^2}_{\text{order 2}} \pm \underbrace{\frac{8}{3}\cos\left(\frac{\pi}{n}\right)\left(\frac{\pi x}{n}\right)^3}_{\text{order 3}} + \ldots$$

$$= 2\sin\left(\frac{\pi}{n}\right) + \frac{1}{2}\sin\left(\frac{\pi}{n}\right)(\omega t_{n,1})^2 \pm \frac{1}{3}\cos\left(\frac{\pi}{n}\right)(\omega t_{n,0})^3 + \ldots$$

$$= 2\sin\left(\frac{\pi}{n}\right) + 2\left(\frac{\omega r}{v}\right)^2 \sin^3\left(\frac{\pi}{n}\right) \pm \frac{8}{3}\left(\frac{\omega r}{v}\right)^3 \cos\left(\frac{\pi}{n}\right)\sin^3\left(\frac{\pi}{n}\right) + \ldots$$

With at order one: $t_{n,1} = t_{n,0} = 2r/v\ \sin(\pi/n)$.

B Relativistic

Slow disk: $v' >> \omega r$, $v \simeq v'$ and $\epsilon = \omega r/v << 1$.
$0 \leqslant \beta = \frac{v_{loc}}{c} = \gamma_D\frac{v}{c} \leqslant 1$, $0 \leqslant \beta_c = \frac{v_{coord}}{c} = \frac{v}{c} \leqslant \beta \leqslant 1$, $\beta_D\beta = \epsilon\beta_c^2$ and $\beta_D = \omega r/c$.
If $\epsilon << 1$ then $\beta_c \simeq \beta$.

$$r^2 = \frac{[v\cos\alpha_n t_n + r(1+\beta_D\beta\sin\alpha_n)]^2 + (\beta\sin\alpha_n + \beta_D)^2 c^2 t_n^2}{(1+\beta_D\beta\sin\alpha_n)^2}$$

$$\text{and} \quad \tan(\pm 2\pi/n + \omega t_n) = \frac{(\beta\sin\alpha_n + \beta_D)ct_n}{v\cos\alpha_n t_n + r(1+\beta_D\beta\sin\alpha_n)}$$

Preprints (www.preprints.org) | NOT PEER-REVIEWED | Posted: 21 November 2022 doi:10.20944/preprints202208.0251.v2

$$\begin{cases} \dfrac{v\cos\alpha_n t_n}{r} = (1+\beta_D\beta\sin\alpha_n)\left(\dfrac{1}{\sqrt{1+\tan^2\theta'_n}}-1\right) & \text{if} \quad n>4 \quad \text{then} \quad x'_n \geqslant 0 \\ \dfrac{v\sin\alpha_n t_n}{r} = \dfrac{1}{\gamma_D}\left(\pm\dfrac{1+\beta_D\beta\sin\alpha_n}{\sqrt{1+1/\tan^2\theta'_n}}-\omega t_n\right) & \text{if} \quad \text{counterclockwise} \quad y'_n \geqslant 0 \quad \text{else} \quad y'_n < 0 \end{cases}$$

$$\omega t_{n,p+1} = \epsilon(1+\beta_D\beta\sin\alpha_{n,p-1})\times \sqrt{\left(\cos\left(\frac{2\pi}{n}\pm\omega t_{n,p}\right)-1\right)^2+\frac{1}{{\gamma_D}^2}\left(\pm\sin\left(\frac{2\pi}{n}\pm\omega t_{n,p}\right)-\frac{\omega t_{n,p}}{1+\beta_D\beta\sin\alpha_{n,p-1}}\right)^2} \quad (27)$$

$$\sin\alpha_{n,p} = \epsilon\frac{1+\beta_D\beta\sin\alpha_{n,p-1}}{\gamma_D\omega t_{n,p+1}}\left(\pm\sin\left(\frac{2\pi}{n}\pm\omega t_{n,p}\right)-\frac{\omega t_{n,p}}{1+\beta_D\beta\sin\alpha_{n,p-1}}\right) \quad (28)$$

$\beta_D\beta = \epsilon{\beta_c}^2\gamma_D$, $\gamma_D = 1/\sqrt{1-\epsilon^2{\beta_c}^2}$ and we consider ωt_n as a function of ϵ.

First non-null orders for a series expansion on ϵ: $\omega t_{n,1} = 2\epsilon\sin\frac{\pi}{n}$ and $\sin\alpha_{n,0} = \pm\cos\frac{\pi}{n}$.
Then with Eq. 27 and $p=1$, we obtain $\omega t_{n,2}$, and with Eq. 28 $\sin\alpha_{n,1}$:
$\omega t_{n,2} = 2\epsilon\sin\frac{\pi}{n} \pm 2\epsilon^2{\beta_c}^2\sin\frac{\pi}{n}\cos\frac{\pi}{n}$ and $\sin\alpha_{n,1} = \pm\cos\frac{\pi}{n} - 2\epsilon\sin^2\frac{\pi}{n}$.
We iterate and we obtain:
$\omega t_{n,3} = \omega t_{n,2} + \epsilon^3\sin\frac{\pi}{n}(2\sin^2\frac{\pi}{n} + {\beta_c}^2(1-5\sin^2\frac{\pi}{n}))$
and $\sin\alpha_{n,2} = \sin\alpha_{n,1} \mp \frac{3}{2}\epsilon^2\sin^2\frac{\pi}{n}\cos\frac{\pi}{n}(2+{\beta_c}^2)$.
Then: $\omega t_{n,4} = \omega t_{n,3} \pm \epsilon^4\sin\frac{\pi}{n}\cos\frac{\pi}{n}[\frac{8}{3}\sin^2\frac{\pi}{n} - 4{\beta_c}^2\sin^2\frac{\pi}{n} - 2{\beta_c}^4(2\sin^2\frac{\pi}{n}-1)]$.